XAFS Analysis for Electrochemical Conversion Process of Manganese Oxide Supported on Carbon

Keiko Fukada, Asaka Azuma and Yasuhiro Inada
Department of Applied Chemistry, Faculty of Life Sciences, Ritsumeikan University, 1-1-1 Noji-Higashi, Kusatsu 525-8577, Japan

Changes in the chemical states of Mn species supported on carbon (Ketjenlack: KB) during drying and calcination were analyzed by X-ray absorption fine structure (XAFS) method. The oxidation reaction of precursor $Mn(NO_3)_2 \cdot 6H_2O$ to MnO_2 was observed with increasing drying period, and MnO_2 was singly supported on KB by the calcination at above 150 °C. The electrode sheet using MnO_2/KB as the active material was prepared and was used in the electrochemical cell with an electrolyte containing Li ions and a counter Li electrode to examine the electrochemical conversion process. The reversible redox cycle of the MnO_2/MnO couple was confirmed by the *in situ* XAFS measurements in the charge-discharge processes, and the excess capacity was considered to be due to the side reactions.

1. Introduction

Lithium-ion rechargeable batteries (LIBs) are widely used in everyday devices such as mobile phones and laptops due to their high energy density and high coulombic efficiency [1]. In recent years, there has been a growing trend toward next-generation LIBs with high capacity and power density developed for electric vehicles [2]. When $LiCoO_2$ and graphite are used as the positive and negative electrode, respectively, lithium ions in the positive electrode are released accompanied by the oxidation of $LiCoO_2$ during the charging process and reach the negative electrode through the electrolyte solution. Lithium ions are reduced and intercalated between the graphite layers to form a Li-graphite intercalation compound [3]. During the discharge process, lithium ions in the Li-graphite intercalation compound are deintercalated and returned to the positive electrode. This reaction is known to have a practical capacity less than 160 mA h g^{-1} [4]. In addition, the use of LIBs is limited because the Li reserves are not as abundant. An electrode reaction system with multiple electron transfer called conversion reaction was discovered in the early 2000s by the research of P. Poizot *et al.* [5]. This is a redox reaction in the solid state with changes in the crystal structure and with the breakage and recombination of chemical bonds. It is expected to solve problems such as energy density limitation for the intercalation reaction. Many transition metal oxides show high theoretical capacity and excellent electrochemical properties [6,7]. On the other hand, the large volume change and voltage hysteresis cause degradation of cycle performance.

The resources of Mn are known to have abundant reserves, low prices, and stable supplies. It is also known that manganese oxide has several oxidation states. MnO_2 is used as a cathode material in various primary batteries such as manganese batteries, alkaline batteries, and manganese lithium batteries [3]. The theoretical capacitances of the MnO_2/Mn, Mn_2O_3/Mn, and Mn_3O_4/Mn couple are 1223, 1018 and 937 mA h g^{-1}, respectively, which are much higher than those of graphite negative electrode (372 mA h g^{-1}). In addition, the reaction voltage for the first discharge process is low (0.2 V to 0.5 V vs. Li^+/Li) and the voltage hysteresis is small (less than 0.8 V) [7]. The electrical conductivity of manganese oxide is extremely low (10^{-7} ~ 10^{-8} S cm^{-1} for Mn_3O_4), which inhibits its use as an electrode material [6]. The general preparation method of electrode mixture is to mix physically particles of the active material with carbon. In this study, the electrode mixture is prepared by supporting manganese oxide particles on carbon using the incipient wetness method. After the prepared active material is characterized by X-ray diffraction (XRD) and X-ray absorption fine structure (XAFS), the conversion battery cell is fabricated, and its charge/discharge characteristics are evaluated. The chemical state change of the Mn species during the charge/discharge process is analyzed by the XAFS method to establish the electrode using conversion reaction using manganese oxide as active material.

2. Experimental

Preparation of MnO_2 Supported on Carbon

Carbon-supported manganese oxide was prepared by the incipient wetness method so that the MnO_2 content was 40 wt%. To 0.5 g of Ketchen Black (KB), 4.5 mL of 0.8 M aqueous solution of $Mn(NO_3)_2 \cdot 6H_2O$ was added dropwise. The mixture was dried at 60 °C by varying the drying period from 12 h to 8 d. The obtained sample after drying for 6 d was calcined under air at 100 °C, 150 °C, and 200 °C for 1 h.

Characterization

The X-ray diffraction (XRD) measurement was performed by MiniFlex600-C (Rigaku) using Cu K_α radiation. The diffraction intensities were recorded in the 2θ values between 10° and 80°. The loading of

the supported Mn species was determined by the X-ray fluorescence analysis (XRF) using the Supermini fluorescent X-ray spectrometer (Rigaku). A calibration curve was obtained using several samples in which a known amount of MnO_2 was physically mixed with KB. The mass change of the prepared sample at the elevated temperature was measured in air using a thermogravimetric and differential thermal analysis (TG-DTA) instrument DTG-60/60H (Shimadzu).

Preparation of Electrode Sheet

To prepare the electrode sheet, 0.204 g of the prepared MnO_2/KB powder and 1.026 g of KF polymer (Kureha) were mixed so that the mass ratio of active material to PVDF was 6:4. 0.810 g of 1-methyl-2-pyrrolidone was added, and the mixture was stirred at 2000 rpm for 20 min using an agitator and defoaming machine. The resultant mixture slurry was coated on an Al foil with a thickness of 488 µm and dried in vacuum at 50 °C for 5 h to obtain the MnO_2/KB electrode sheet.

Fabrication of Electrochemical Cell

The electrochemical cell using an Al-coated laminate film was assembled to perform electrochemical measurements using the prepared MnO_2/KB electrode. The MnO_2/KB electrode sheet welded with an Al tab, a porous polypropylene film as the separator, and the Ni tab for the counter Li electrode were sandwiched by 2 sheets of laminate film. This assembly was vacuum-dried at 100 °C for 1 h and introduced into a glove box under an Ar atmosphere. Li foil was crimped to the Ni tab in the glove box. 100 µL of 1 M $LiPF_6$ solution dissolved in a 1:1 mixture of ethylene carbonate and diethyl carbonate was soaked into the separator, and 2 sides were closed with a sealer. Finally, another 200 µL of $LiPF_6$ solution was added, and the last side was closed and sealed.

XAFS Measurements

The XAFS measurements were carried out at the Mn K edge in transmission mode using a Si(220) double-crystal monochromators at BL-3 of the SR Center (Ritsumeikan Univ.). The amount of powder samples required for the XAFS measurement was estimated based on the absorption coefficient and the tablet was prepared with a diameter of 10 mm by mixing with BN powder. The electrochemical cell was used for *in-situ* XAFS measurements after the discharge and charge processes.

The linear combination fitting (LCF) analysis was performed using the observed X-ray absorption near edge structure (XANES) spectrum to determine the sample composition.

3. Results and Discussion

3.1. Analysis of Prepared Sample

The XRD patterns of the KB-supported samples dried at 60 °C for various drying periods are shown in Fig. 1. No diffraction peaks were detected for the samples dried for less than 1 d, and the XRD pattern of the other samples almost agreed with that of β-MnO_2 [8]. Therefore, the samples dried for more than 2 d were identified as β-MnO_2/KB. It should be noted that a diffraction line at 28.69° assigned to the (110) plane was not observed in the prepared samples suggesting the slow growth of the (110) plane.

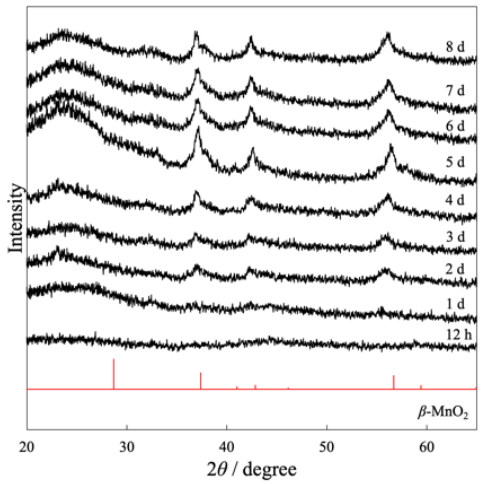

Fig. 1. XRD patterns of KB-supported samples dried for various periods.

The XANES change for all dried samples are shown in Fig. 2 together with the XANES spectra of MnO_2, Mn_2O_3, Mn_3O_4, and $Mn(NO_3)_2 \cdot 6H_2O$. The XANES spectrum of sample dried for 12 h agreed with that of $Mn(NO_3)_2 \cdot 6H_2O$ with the intense white line at 6.548 keV, indicating that the precursor

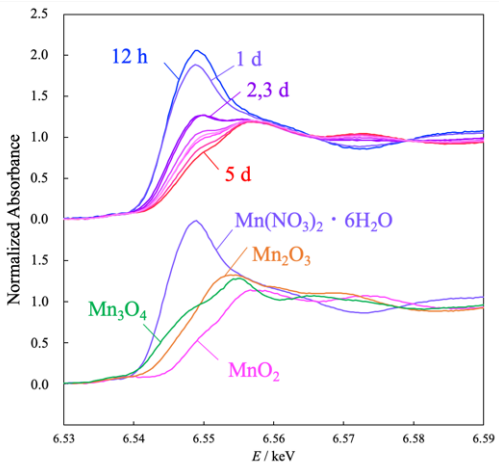

Fig. 2. XANES spectral change of KB-supported samples dried for various periods.

$Mn(NO_3)_2 \cdot 6H_2O$ was initially supported on KB. The absorbance at 6.548 keV was decreased with increasing the drying time. The observed spectrum of samples dried over 1 d was not in agreement with the spectrum of any standard sample, thus it could be identified as the mixture of some species. Because the XANES spectrum of the KB-supported sample dried for 6 d was well reproduced by the LCF analysis using $Mn(NO_3)_2 \cdot 6H_2O$ and MnO_2, the compositions for all samples were evaluated as shown in Fig. 3. It was found that increasing the drying time at 60 °C progressed the oxidation of the precursor $Mn(NO_3)_2 \cdot 6H_2O$ to MnO_2. This result is similar to that reported previously on silica but is contrast to that observed on activated carbon, where the formation of MnO_2 was followed by reduction to Mn_2O_3 [9].

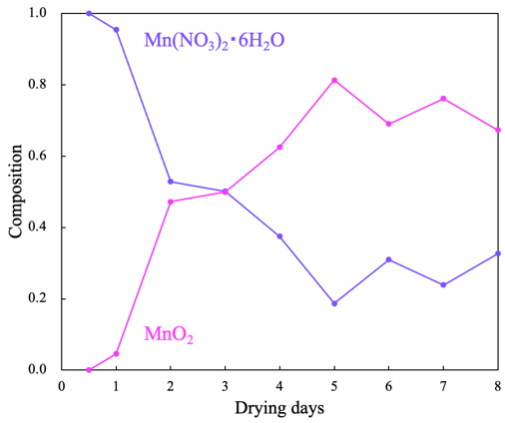

Fig. 3. Change in composition of the KB-supported Mn species during the drying process.

The TG data for the KB-supported sample dried at 60 °C for 12 h is given in Fig. 4. The sample weight changed below 150 °C and remained almost constant in the temperature range from 150 to 250 °C.

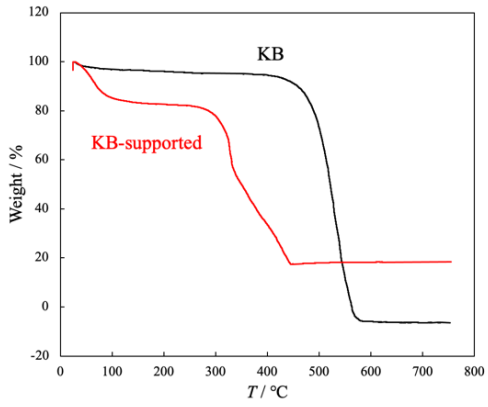

Fig. 4. TG data for the KB-supported sample dried for 12 h compared with that of KB alone.

Considering the change in chemical state during the drying process described above, the formation of MnO_2/KB is expected in the temperature range where the mass becomes constant. The sudden mass loss at 300 °C was a large exothermic process, and thus the KB combustion is expected. The corresponding combustion of KB alone was observed at 540 °C, and the combustion temperature was shifted to lower by supporting MnO_2, indicating the catalysis by MnO_2 for carbon combustion.

Figure 5 shows the XRD patterns of samples dried at 60 °C for 6 d and calcined in air at 100 °C, 150 °C, and 200 °C. All calcined samples exhibited the XRD pattern consistent with β-MnO_2. The XANES spectra at the Mn K edge of these samples are shown in Fig. 6 compared with those of MnO_2, Mn_2O_3, Mn_3O_4 and $Mn(NO_3)_2 \cdot 6H_2O$. The XANES spectra of the samples after the calcination at 150 °C and 200 °C are in good agreement with MnO_2, whereas the sample calcined at 100 °C has slightly high

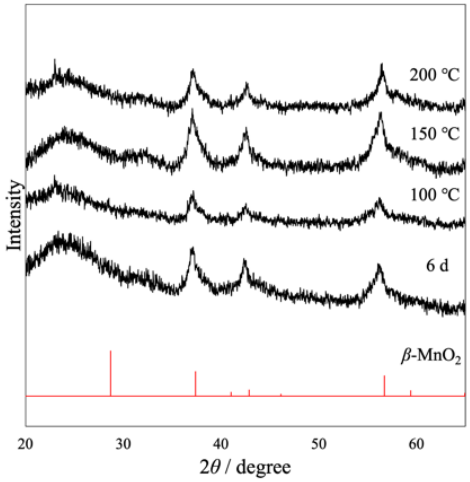

Fig. 5. XRD patterns of KB-supported samples after the calcination in air at various temperature.

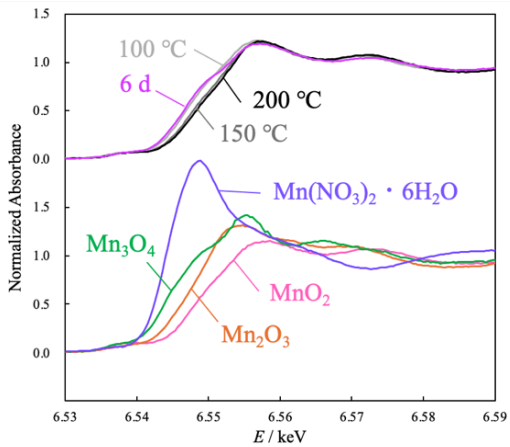

Fig. 6. XANES spectra of KB-supported samples after the calcination in air at various temperature.

absorbance around 6.548 keV, suggesting that the $Mn(NO_3)_2 \cdot 6H_2O$ precursor still remains. The present characterizations revealed that MnO_2 was possible to be supported on KB as a single species by the dry at 60 °C and the calcination at 200 °C in air. By the XRF analysis using standard samples prepared by mixing MnO_2 and KB in known masses, the loading of MnO_2 in the prepared sample was determined to be 42.7 wt%.

3.2. Analysis of Battery Electrode

The constant-current charge-discharge test was conducted for the fabricated electrochemical cell with the MnO_2/KB electrode in the voltage range from 0.4 V (discharge) to 4.1 V (charge) vs. Li^+/Li under the current density of 61.7 mA g^{-1}. The observed charge-discharge curves for three cycles are shown in Fig. 7. During the first discharge process, the battery showed voltage plateaus at 2.7 V, 1.1 V, and 0.9 V, with a capacity exceeding 2300 mA h g^{-1} at 0.4 V. The capacity of the first charge was approximately 1800 mA h g^{-1} at 4.1 V, and the battery showed voltage plateaus at 1.7 V and 3.2 V. In the two subsequent charge-discharge cycles, the plateau voltages did not appear clearly, but the reversible charge-discharge process proceeded with each capacity being almost maintained.

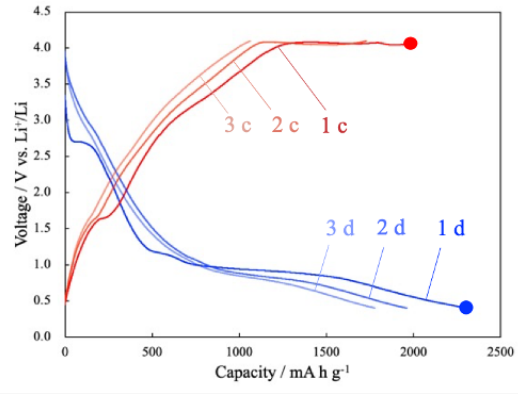

Fig. 7. The discharge (1d, 2d, and 3d) and charge (1c, 2c, and 3c) curves for three cycles under the current density of 61.7 mA g^{-1}. The XAFS measurements have been carried out at the final stages of the first discharge and charge process denoted by circle points.

Previous study on a similarly configured battery using nanowire-type γ-MnO_2 electrode reported a continuous voltage drop from 3.0 to 0.5 V vs Li^+/Li during the first discharge, followed by a plateau with high capacity at 0.4 V, resulting in the discharge capacity of 1700 mA h g^{-1} [10]. During the subsequent charging process, a capacity of about 700 mA h g^{-1} was observed up to 1.4 V, and then a second anodic reaction proceeded in the voltage range from 2.5 to 2.8 V, resulting in the charge capacity of 1200 mA h g^{-1}. Similar charge-discharge curves have been reported for batteries using interconnected nanowire [11] and nanoporous [12] MnO_2 as the active material. In the case of MnO_2 supported on KB used in this study, voltage characteristics approximately 0.5 V higher were observed during both the discharge and charge processes. To analyze the change in the chemical state of the Mn species supported on KB, *in situ* XAFS measurements were performed for the batteries at the final stages of the first discharge and charge process, which are indicated by the circle points in Fig 7.

The XANES spectra of the MnO_2/KB electrode obtained by *in situ* XAFS measurements after the first discharge process and the subsequent charge process are shown in Fig. 8 together with that of the initial battery. As shown in the above discussion, the Mn species in the electrodes in the initial battery was consistent with MnO_2, and there was no change in the chemical state when immersed in the electrolyte. After the first discharge to 0.4 V vs. Li^+/Li, the absorption edge energy shifted to lower by *ca*. 9 eV, confirming the progress of the reduction reaction of MnO_2. The XAFS analysis in this study revealed that the reduction of MnO_2 to MnO proceeded, based on comparison with standard samples. Furthermore, the XANES spectrum after the subsequent charge process was in good agreement with that of the initial battery, revealing that MnO was quantitatively oxidized to MnO_2. The present XAFS analysis clearly revealed that a reversible conversion reaction between MnO_2 and MnO occurred during the charge and discharge process in the range of 0.4 to 4.1 V vs. Li^+/Li. The theoretical capacity of the MnO_2/MnO

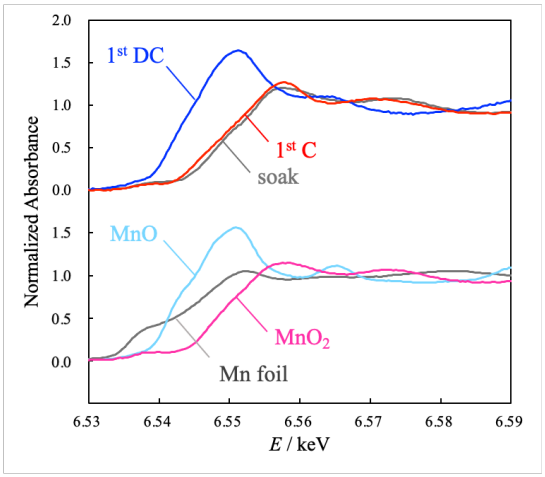

Fig. 8. XANES spectra of MnO_2/KB electrode obtained by the *in situ* XAFS measurements after the first discharge (1d) and first charge (1c). For comparison, the XANES spectra of the initial battery (soak) and reference samples were included.

couple for the two-electron redox reaction is calculated to be 617 mA h g^{-1}. The observed capacities shown in Fig. 7 are in excess during both the discharge and charge processes, implying that there is a contribution from other than the conversion reaction between MnO_2 and MnO. An environment is required in which the oxide ions released during the conversion from MnO_2 to MnO can be stored within the electrode, and an appropriate supply of oxide ions is required when MnO reverts to MnO_2. The presence of solid-electrolyte interphase has been pointed out as such an environment in electrodes that use a conversion process of metal oxides [13-16], and it is considered that excess capacity is used for the decomposition of electrolyte components to generate the solid-electrolyte interphase.

4. Conclusions

In this study, KB-supported MnO_2 was prepared by the incipient wetness method using $Mn(NO_3)_2 \cdot 6H_2O$ as a precursor. XRD and XAFS measurements were performed to analyze the changes in the state of the prepared samples when the drying period and the calcination temperature were varied. The XAFS analysis revealed that $Mn(NO_3)_2 \cdot 6H_2O$ was initially supported by drying at 60 °C and that the oxidation to MnO_2 progressed as the drying period was extended. Furthermore, it was confirmed that $Mn(NO_3)_2 \cdot 6H_2O$ was quantitatively converted to MnO_2 by the calcination at 200 °C in air. The electrode was fabricated using the obtained MnO_2/KB as the active material, and the electrochemical cell with a Li counter electrode was assembled to examine the charge-discharge characteristics and to perform *in situ* XAFS measurements. The XAFS analysis revealed that the two-electron redox reaction between MnO_2 and MnO reversibly cycled during the charge and discharge process. The charge-discharge capacity of the MnO_2/KB electrode prepared in this study exceeded the theoretical capacity of the MnO_2/MnO couple, which suggests that side reactions such as the formation of solid-electrolyte interphase are taking place simultaneously. In future research, we intend to analyze the detailed chemical state changes during the charge-discharge process using *in situ* XAFS measurements and other techniques.

References

[1] Y. Chen, X. Chen, and Y. Zhang, *Energy Fuels*, **2021**, *35*, 6420.
[2] T. Kim, W. Song, D.-Y. Son, L. K. Ono, and Y. Qi, *J. Mater. Chem. A*, **2019**, *7*, 2942.
[3] V. Aravindan, Y.-S. Lee, and S. Madhavi, *Adv. Energy Mater.*, **2015**, *13*, 1402225.
[4] A. Manthiram, *J. Phys. Chem. Lett.*, **2011**, *2*, 176.
[5] P. Poizot, S. Laruelle, S. Grugeon, L. Dupont, and J.-M. Tarascon, *Nature*, **2000**, *407*, 496.
[6] S.-H. Yu, S. H. Lee, D. J. Lee, Y.-E. Sung, and T. Hyeon, *Small*, **2016**,*12*, 2146.
[7] J. Cabana, L. Monconduit, D. Larcher, and M. R. Palacín, *Adv. Mater.*, **2010**, *22*, E170.
[8] N. Curetti, M. Merli, S. Capella, P. Benna, and A. Pavese, *Phys. Chem. Miner.*, **2019**, *46*, 987.
[9] A. Azuma, K. Fukada, M. Katayama, and Y. Inada, *Mem. SR Center Ritsumeikan Univ.*, **2024**, *26*, 8.
[10] M.-S. Wu and P.-C. J. Chiang, *Electrochem. Commun.*, **2006**, *8*, 383.
[11] M.-S. Wu, P.-C. J. Chiang, J.-T. Lee, and J.-C. Lin, *J. Phys. Chem. B*, **2005**, *109*, 23279.
[12] J. Zhao, Z. Tao, J. Liang, and J. Chen, *Cryst. Growth Design*, **2008**, *8*, 2799.
[13] J. G. Thevenin and R. H. Muller, *J. Electrochem. Soc.*, **1987**, *134*, 273.
[14] S. Laruelle, S. Grugeon, P. Poizot, M. Dolle, L. Dupont, and J.-M. Tarascon, *J. Electrochem. Soc.*, **2002**, *149*, A627.
[15] D. Aurbach, *J. Power Sources*, **2006**, *153*, 380.
[16] H. Liu, G. Wang, J. Liu, S. Qiao, and H. Ahn, *J. Mater. Chem.*, **2011**, *21*, 3046.